Lawrence Berkeley National Laboratory
Lawrence Berkeley National Laboratory

Title

Remediation of Cr(VI) by biogenic magnetic nanoparticles: An x-ray magnetic circular dichroism study

Permalink

Author

Telling, N. D.

Publication Date

Peer reviewed

Remediation of Cr(VI) by biogenic magnetic nanoparticles: An x-ray magnetic circular dichroism study

N. D. Telling[1], V. S. Coker[1], R. S. Cutting[1], G. van der Laan[1,2], C. I. Pearce[1], R. A. D. Pattrick[1], E. Arenholz[3], and J. R. Lloyd[1]

[1]*School of Earth, Atmospheric and Environmental Sciences, University of Manchester, Manchester M13 9PL, UK*

[2]*Magnetic Spectroscopy Group, Diamond Light Source, Didcot, Oxfordshire, OX11 0DE, UK*

[3]*Advanced Light Source, Lawrence Berkeley National Laboratory, Berkeley, CA, USA*

Biologically synthesized magnetite (Fe_3O_4) nanoparticles are studied using x-ray absorption and x-ray magnetic circular dichroism following exposure to hexavalent Cr solution. By examining their magnetic state, Cr cations are shown to exist in trivalent form on octahedral sites within the magnetite spinel surface. The possibility of reducing toxic Cr(VI) into a stable, non-toxic form, such as a Cr^{3+}-spinel layer, makes biogenic magnetite nanoparticles an attractive candidate for Cr remediation.

Magnetic nanoparticles have potential applications in areas as diverse as cancer therapies[1] and magnetoelectronic devices[2,3]. Their enhanced surface catalytic properties also make them very suitable for oxidation-reduction (redox) reactions[3]. One such reaction that has important environmental and health consequences involves the reduction and immobilization of highly toxic Cr^{6+} cations, found in Cr contaminated groundwaters, to their less harmful Cr^{3+} counterpart[4,5]. In this Letter we describe the use of x-ray absorption (XA) and x-ray magnetic circular dichroism (XMCD) to probe the near surface region of biologically synthesized (biogenic) magnetite nanoparticles, following exposure to varying concentrations of Cr^{6+} containing solution. Biogenic magnetite offers a route to the scaled-up nanoparticle production required for Cr remediation, whilst using environmentally friendly preparation methods. Previous Cr remediation studies using synthetic zero-valent Fe and iron oxide surfaces suggested the formation of Cr^{3+}-rich oxide and oxy-hydroxide surface layers[4-6]. In contrast, the results presented here indicate the incorporation of Cr^{3+} cations into octahedral sites of the magnetite spinel structure.

Highly crystalline biogenic magnetite nanoparticles with average dimensions of ~20 nm were obtained from a ferrihydrite suspension starting material using the bacterium *Geobacter sulfurreducens*, as described in detail elsewhere[7,8]. The nanoparticles were subsequently exposed to a solution of Cr(VI) (potassium chromate) at varying concentrations of 0.5 mM, 1 mM, and 5 mM [8]. Batch chromate reduction experiments clearly showed that the biogenic magnetite nanoparticles were successful at reducing Cr(VI) for all concentrations used[8]. XA and XMCD measurements were performed on untreated and Cr-exposed samples, using beamline 4.0.2 at the Advanced Light Source, Lawrence Berkeley National Laboratory. Spectra were obtained using total-electron-yield detection, which gives a probing depth of ~4 nm. Care was taken to ensure that the nanoparticles were maintained in anaerobic conditions at all stages of the experiment by placing them in airtight containers for transport and performing sample handling only in anaerobic environments.

The XA spectra measured across the Cr and Fe $L_{2,3}$ edges for the Cr treated nanoparticles are shown in Fig. 1. From the relative heights of the main Cr and Fe L_3 absorption peaks, the deduced Cr content in the nanoparticles displays a scaling behaviour with increasing Cr(VI) concentration, consistent with previous studies on magnetite surfaces reacted with Cr solution[6]. In addition, a shoulder feature at ~708 eV on the Fe main absorption feature develops with increasing Cr content (Fig. 1)

indicating the surface oxidation of magnetite Fe^{2+} cations to Fe^{3+} [9], which is an expected consequence of the redox reaction with Cr(VI) solution. The same Fe^{3+} enrichment would also be seen by substituting Fe^{2+} cations by Cr.

The Cr XA spectrum for the sample treated with 5 mM Cr(VI) solutions is compared to standard compounds in Fig. 2(a). Samples treated with lower Cr(VI) concentrations displayed almost identical spectra. It can be seen that the nanoparticle spectrum is very similar to that obtained from the trivalent Cr compound and varies greatly from the Cr^{6+} containing compound. There is no obvious contribution from Cr^{6+} to the XA spectrum, suggesting that the surface contains predominately Cr^{3+} cations. Furthermore, the XA spectral shape indicates an octahedral site symmetry for the Cr cations[6,10,11], in agreement with the strong site preference due to the favourable fit of the charge distribution of the Cr^{3+} ions in the crystal field at an octahedral site.

A more quantitative analysis can be performed using XMCD, i.e. the difference of XA spectra measured using circularly polarized x-rays in a 0.6 T magnetic field applied parallel and antiparallel to the x-ray beam direction. The XMCD spectra for the Cr-treated nanoparticles are shown in Fig. 2(b). A clear dichroism is observed for all the samples, indicating the presence of magnetic Cr cations in the nanoparticle surface region. The sign of the Cr XMCD signal compared to that of the Fe confirms the octahedral site occupation. The XMCD spectra shown in Fig. 2(b) are almost identical to those measured from $CrFe_2O_4$ spinel ferrite powders[11], and are well reproduced by a multiplet calculation using a charge-transfer model with trivalent Cr cations on octahedral sites (Fig. 2(b)). The close similarity of the XMCD obtained here with that presented in Ref. 11 would thus imply that at least some of the Cr must be incorporated into the magnetite spinel structure. However, it can also be seen from Fig. 2(b) that the relative strength of the XMCD signal is weaker for higher Cr-content samples. Thus only a portion of the Cr is able to incorporate into the spinel structure and so to become magnetically polarized. Additonal Cr must reside in non-magnetic (or antiferromagnetic) Cr^{3+}-rich surface phases, in agreement with previous observations[4-6]

The Fe cation site occupation in the nanoparticles was investigated by analyzing the Fe $L_{2,3}$ XMCD. Spectra obtained over the L_3 absorption region are shown for as-prepared and Cr-treated samples in Fig. 3(a). The XMCD is the sum of the contributions from the possible cation sites[7,12] where the most intense negative and positive peaks correspond to the Fe^{2+} and Fe^{3+} octahedral (Oh) and Fe^{3+} tetrahedral

(Td) cation sites, respectively (see Fig. 3(a) for a peak assignment). It appears that the effect of Cr treatment is to remove Fe^{2+} cations in Oh sites, as indicated by the reduction in the first negative peak. However a comparison with the XMCD obtained for Co-doped magnetite nanoparticles in which only removal of Fe^{2+} cations occurs (Fig. 3(b)),[7] reveals an additional enhancement of the positive peak. This is due to the spectral overlap of the components in the XMCD spectrum such that a decrease in Fe^{2+} Oh leads to a more pronounced Fe^{3+} Td peak.

The Fe L_3 XMCD spectra were fitted using the weighted sum of the theoretically calculated spectra for each Fe site as shown in Fig. 4. As there is no evidence of changes in the tetrahedral site occupation following reaction with Cr in either this experiment or previous work, the Fe^{3+} Td component was fixed in the fitting procedure. From the fitted components shown in Fig. 4(b,c) for the XMCD it can be seen that the reaction with Cr solution decreases the Fe^{2+} site occupancy, *and* increases Fe^{3+} occupancy, but by unequal amounts. Thus it appears that both Cr^{3+} incorporation on Fe^{2+} sites and cation oxidation from Fe^{2+} to Fe^{3+} has occurred. The change in Fe^{2+} and Fe^{3+} occupancy as a function of Cr(VI) concentration for the entire sample series is shown in Fig. 5(a). Their net difference in Fig. 5(b) gives an indication of the Cr occupancy. It can be seen from Fig. 5(b) that Cr is incorporated into the spinel structure even at low initial Cr(VI) concentrations, as was also found from the Cr $L_{2,3}$ XMCD spectra. However, significant oxidation of the magnetite was only observed for the sample treated with 5 mM concentration of Cr(VI) solution.

In summary, we have used XA and XMCD at the Fe and Cr $L_{2,3}$ edges to probe biogenic magnetite nanoparticles following redox reactions with Cr(VI) solution. The results show the presence of magnetically polarized Cr^{3+} cations and indicate the incorporation of Cr into octahedral sites in the spinel near surface region. Higher Cr concentrations lead to the additional formation of Cr-rich surface layers, as found in previous studies[4-6]. Analysis of the Fe XMCD spectra enabled us to distinguish between Fe^{2+} cations replaced due to Cr substitution, and those oxidized to Fe^{3+}. The ability of the nanoparticles to fully incorporate Cr into a stable spinel structure at low Cr(VI) concentrations has huge implications for environmental applications such as ground water remediation, where the hexavalent Cr concentration is likely to be even lower than that used in this study.

1. G. F. Goya, V. Grazú, and M. R. Ibarra, Curr. Nanoscience **4**, 1 (2008).

2. W. Wang, M. Yu, M. Batzill, J. He, U. Diebold, and J. Tang, Phys. Rev. B **73**, 134412 (2006).

3. Y-w. Jun, J-s. Choi, and J. Cheon, Chem. Commun. **12**, 1203 (2007),

4. M. L. Peterson, A. F. White, G. E. Brown, Jr., and G. A. Parks, Environ. Sci. Technol. **31**, 1573 (1997).

5. B. A. Manning, J. R. Kiser, H. Kwon, and S. R. Kanel, Environ. Sci. Technol. **41**, 586 (2007).

6. T. Kendelewicz, P. Liu. C. S. Doyle, G. E. Brown, Jr., E. J. Nelson, and S. A. Chambers, Surf. Sci. **424**, 219 (1999).

7. V. S. Coker, N. D. Telling, G. van der Laan, R. A. D. Pattrick, C. I. Pearce, E. Arenholz, F. Tuna, R. E. P. Winpenny, and J. R. Lloyd, ACS Nano **3**, 1922 (2009).

8. R. S. Cutting, V. S. Coker, N. D. Telling, R. L. Kimber, C. I. Pearce, B. Ellis, R. Lawson, G. van der Laan, R. A. D. Pattrick, D. J. Vaughan, E. Arenholz, and J. R. Lloyd, Environ. Sci. Technol., submitted (2009).

9. S. J. Brotton, R. Shapiro, G. van der Laan, J. Guo, P. A. Glans, and J. M. Ajello, J. Geophys. Res. **112**, G03004 (2007).

10. G. van der Laan and I. W. Kirkman, J. Phys.: Condens. Matter **4**, 4189 (1992).

11. M. Mizumaki, A. Agui, Y. Saitoh, M. Nakazawa, T. Matsushita, and A. Kotani, Surf. Rev. Lett. **9**, 849 (2002).

12. R. A. D. Pattrick, G. van der Laan, C. M. B. Henderson, P. Kuiper, E. Dudzik, and D. J. Vaughan, Eur. J. Mineral. **14,** 1095 (2002).

Figure captions

FIG. 1: XA spectra of the Cr and Fe $L_{2,3}$ edges for magnetite nanoparticles treated with solutions of varying Cr(VI) concentration.

FIG. 2: (color online) (a) Cr $L_{2,3}$ XA spectra for nanoparticles treated with 5 mM solution (top) compared to standards obtained from ref. 6. (b) XMCD spectra for nanoparticles treated with solutions of varying Cr(VI) concentration (top). The XMCD spectra were obtained after first normalising the (background subtracted) XA spectra to unity at the L_3 maximum. The lower curve is a charge transfer multiplet calculation reproduced from ref. 11.

FIG. 3: (color online) Fe L_3 XMCD measured from untreated magnetite nanoparticles (dashed blue curve) compared to (a) nanoparticles treated with 5 mM Cr(VI) solution and (b) Co doped magnetite nanoparticles (red solid curves). The data in (b) is taken from Ref. 7.

FIG. 4: (color online) (a) Fe $L_{2,3}$ XMCD spectra measured from untreated and Cr(VI) reacted magnetite nanoparticles (black circles) together with corresponding best-fit curves (red drawn curves). The corresponding scaled cation site components used for the best-fit curves are shown in (b) and (c).

FIG. 5: (color online) (a) Change in Fe^{3+} and Fe^{2+} octahedral (Oh) site occupancy relative to the untreated sample, determined from fitting the XMCD spectra. (b) Net change in Fe^{2+} Oh occupation (corrected for oxidation $Fe^{2+} \rightarrow Fe^{3+}$), obtained by the sum of the curves in (a). Lines are guides to the eye.
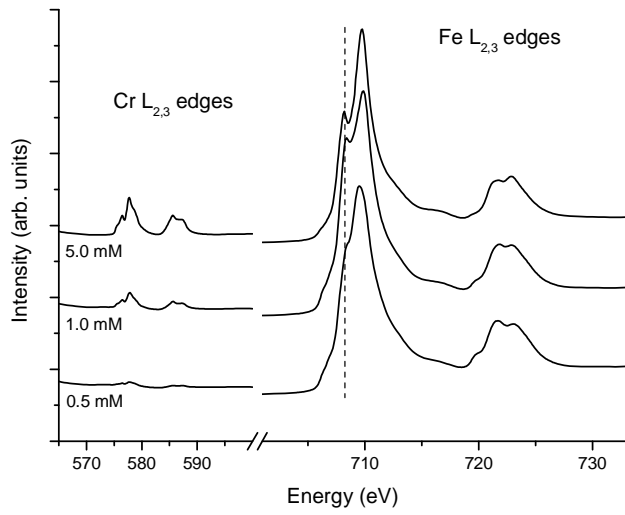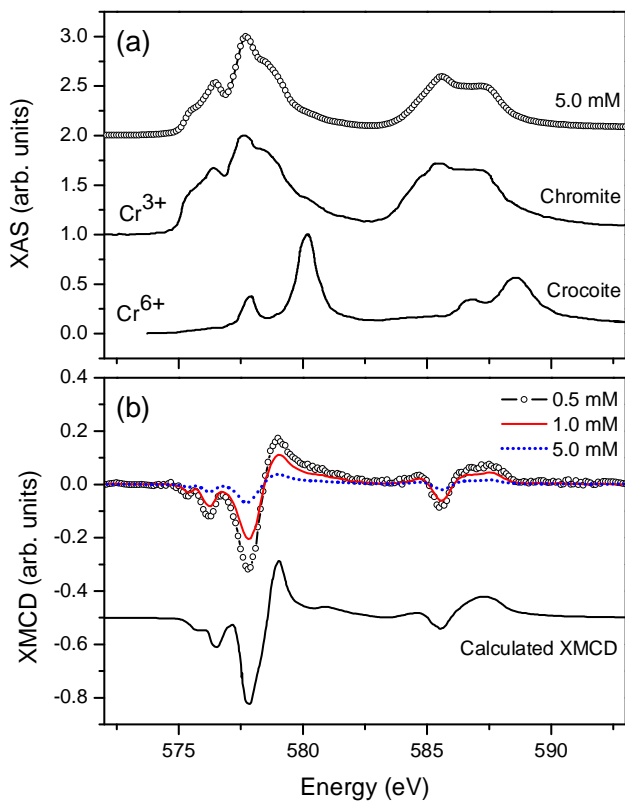
Fig. 1

Fig. 2

Fig. 3

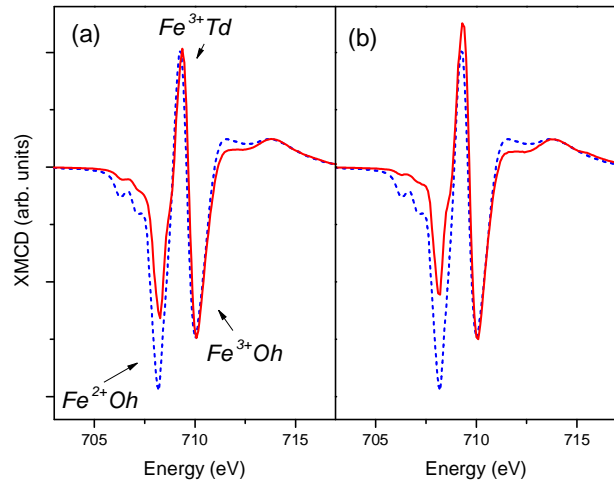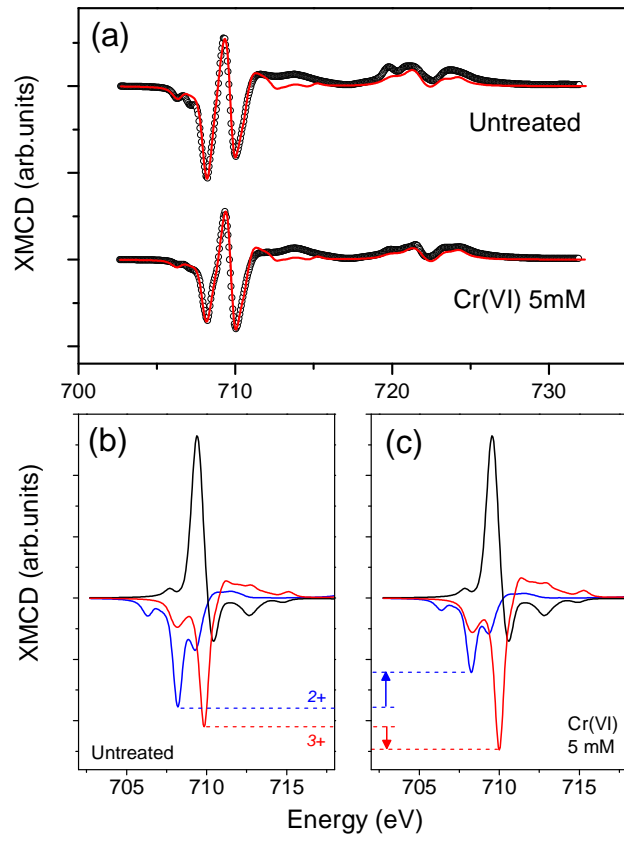Fig. 4

Fig. 5